

Bone tissue formation in sheep muscles induced by a biphasic calcium phosphate ceramic and fibrin glue composite

Damien Le Nihouannen · Afchine Saffarzadeh ·
Olivier Gauthier · Françoise Moreau · Paul Pilet ·
Reiner Spaethe · Pierre Layrolle · Guy Daculsi

Received: 21 April 2006 / Accepted: 25 July 2006 / Published online: 10 July 2007
© Springer Science+Business Media, LLC 2007

Abstract Some biomaterials are able to induce ectopic bone formation in muscles of large animals. The osteoinductive potential of macro- micro-porous biphasic calcium phosphate (MBCP) ceramic granules with fibrin glue was evaluated by intramuscular implantation for 6 months in six adult female sheep. The MBCP granules were 1–2 mm in size and were composed of hydroxyapatite (HA) and beta-tricalcium phosphate (β -TCP) in a 60/40 ratio. The fibrin glue was composed of fibrinogen, thrombin and other biological factors. After 6 months of implantation in the dorsal muscles of sheep, the explants were rigid. Histology, back-scattered electron microscopy and micro-computed tomography of the implants indicated that approximately 12% of mineralized bone had formed in between the MBCP granules. The ectopic bone appeared well-mineralized with mature osteocytes and Haversian structures. In addition, the number and thickness of bone trabeculae formed in between the MBCP particles were similar to those measured in trabecular bone in sheep. The overall

results therefore confirmed the formation of well-mineralized ectopic bone tissue after intramuscular implantation of MBCP/fibrin glue composites. These bone substitutes exhibiting osteoinductive properties could be used for the reconstruction of large bone defects.

Introduction

Many clinical indications, such as spine fusion, orthopedic, cranial and maxillo-facial surgery, require bone graft materials for the reconstruction of large bone defects [1]. Autologous bone remains the gold standard in bone reconstructive surgery because of its osteogenic properties. However, bone autografts are limited in quantity (about 20 cm³), often associated with complications at the harvesting site (iliac crest) and hazardous viability because of the lack of blood supply [1]. Bone allografts, including demineralized bone matrix (DBM) have osteogenic properties that are inferior to those of autologous bone and might lead to the transmission of disease or immunological reactions [2]. Synthetic bone substitutes, mainly calcium phosphate ceramics, are used increasingly in spinal, orthopedic and maxillo-facial surgery. These materials are bioactive and osteoconductive, forming a direct bond with living bone tissue [3]. Depending on their composition and structure, bioceramics degrade and are gradually replaced by bone. However, calcium phosphate ceramics generally lack the osteogenic property for promoting bone healing over large or critical-sized bone defects. Certain calcium phosphate bioceramics have recently been shown to induce ectopic bone formation [4–6]. These animal studies have demonstrated that bioceramics should have a micro- and

D. Le Nihouannen · A. Saffarzadeh · O. Gauthier ·
F. Moreau · P. Pilet · P. Layrolle (✉) · G. Daculsi
Inserm, U791, Laboratoire d'ingénierie ostéoarticulaire et
dentaire, Univ Nantes, Faculté de chirurgie dentaire,
1 place Alexis Ricordeau, Nantes 44042, France
e-mail: pierre.layrolle@univ-nantes.fr

O. Gauthier
Ecole Nationale Vétérinaire de Nantes, Service de chirurgie,
route de Gachet, Nantes 44307, France

P. Pilet
Inserm RIO IFR 26 – 1, place Alexis Ricordeau, Nantes 44042,
France

R. Spaethe
Baxter BioSciences BioSurgery, Vienna, Austria

macro-porous structure in order to form mineralized bone in ectopic sites after a few weeks. Nevertheless, material osteogenesis has been found to be animal-dependent and so far, it has only been observed in the muscles or subcutis of large animals [5–10]. The biological mechanism leading to osteoinduction by biomaterials has not yet been identified and several hypotheses have been proposed [3, 6, 11].

Fibrin glues, mainly composed of fibrinogen and thrombin, mimic the final stage of blood clotting. Thanks to their hemostatic, mitogenic and angiogenic properties, fibrin glues are widely used in surgery [12]. Fibrin glues are usually sprayed over the wound in order to prevent blood loss. They are well known for their wound healing and tissue regeneration properties, but their use as a bone graft material has been infrequent [13–15]. Only a few publications have reported the osteoinductive properties of fibrin glues [16, 17].

The association of calcium phosphate bioceramics and fibrin glues has led to composite biomaterials with new biomechanical properties. The resulting bioceramic–fibrin composite has already demonstrated its ability to fill bone defects and promote bone healing in numerous *in vivo* and clinical studies [18–25]. Moreover, mixtures of bioceramic and fibrin glue have also been proposed as scaffolds for bone tissue engineering in association with mesenchymal stem cells. The composite scaffolds have been shown to support the proliferation and differentiation of mesenchymal stem cells and to induce bone tissue formation *in vitro* as well as *in vivo* in small animal models [26–29]. However, the osteoinductive properties of calcium phosphate bioceramic and fibrin glue composites, without the addition of mesenchymal stem cells or osteogenic factors, have not been studied.

The aim of this study was to investigate the osteoinductive potential of macro-/micro-porous biphasic calcium phosphate (MBCP) ceramic particles associated with fibrin glue. The MBCP ceramic granules mixed with fibrin glue were implanted into the lumbar muscles of sheep for 6 months. After euthanasia, the implants were analyzed histologically, with back-scattered electron microscopy and micro-computed tomography techniques.

Materials and methods

Materials

Microporous biphasic calcium phosphate granules (MBCP, TricOs[®], Baxter BioSciences BioSurgery, Vienna Austria) measuring 1–2 mm in diameter and having a 60/40 hydroxyapatite/ β -tricalcium phosphate weight ratio were used. The MBCP granules were prepared by mixing calcium-deficient apatite with pore

makers, followed by compaction and sintering at 1,050 °C. The chemical purity of the MBCP was analyzed by X-ray diffraction (XRD, Philips PW 1830, CuK α source) and Fourier transform infrared spectroscopy (FTIR, Nicolet, Magna-IR 550). Finally, a phenolphthalein test was used to check for traces of CaO in the MBCP. The macroporosity was about 45% with macropores in the 260–550 μ m size range. The microporosity was approximately 25% including micropores less than 10 μ m in size. The macro- and micro-porosity were measured using a mercury intrusion porosimeter (AutoPoreIII, Micromeritics). The specific surface area of the MBCP was determined using the Brunauer–Emmett–Teller (BET) method with helium adsorption–desorption (Micromeritics). Two cm³ of MBCP granules were packaged into a syringe and sterilized by γ radiation (>25 kGy).

The fibrin sealant used in this study was Tissucol[®] kit (Baxter AG, Austria). The fibrin sealant was prepared for a final concentration in the thrombin solution of 4 IU. The preparation of the composite was done according to the instructions for use from the manufacturer (TricOs/Tissucol composite). Briefly, sterile water (1.5 mL) was first injected in a custom-made syringe containing the MBCP granules and any excess water was removed. The composite was then prepared by simultaneously injecting and mixing the two-fibrin components, namely 1 mL of fibrinogen and 1 mL of thrombin with the 2 cm³ of the granules. About 2–3 cm³ of the ceramic granules/polymer sealant composite were obtained and readily implanted into the sheep muscles.

Surgical procedure

All animal handling and surgical procedures were conducted according to European Community guidelines for the care and use of laboratory animals (DE 86/609/CEE) and approved by the local Veterinary School ethical committee. Six adult female sheep with an average weight of 64 kg were used in this study. All surgical procedures were performed under general anesthesia induced with intravenous diazepam (1 mg/kg) and ketamine (8 mg/kg) and followed by volatile anesthesia with oxygen and halothane. During surgery, the animals received an intravenous saline isotonic solution (NaCl 0.9%) and 1 g of amoxicillin through a catheter in the jugular vein. For the intramuscular implantation, the lumbar regions were shaved and disinfected with iodine. Each animal received one implant bilaterally in the erector spinae muscles (*luggissimus lumborum*). Two skin and muscle incisions were made on each side of the spine, approximately 5 cm from the median axis of the spine. After incision of the skin and muscular fascia, the lumbar muscles were separated to provide an

intramuscular space with a cranio-caudal direction parallel to the spinal axis. The extremity of the syringe containing the MBCP/fibrin sealant composite was cut and the excess fibrin sealant removed. About 2–3 cm³ of composite biomaterials were implanted into lumbar muscles. After implantation of the materials, the wound and skin flaps were immediately closed in two layers using resorbable sutures (Vicryl[®] 4-0, Johnson & Johnson Intl). After surgery, the animals received one antibiotic (amoxicillin, i.v. injection 2 g/day) for 5 days and clinical follow-up was performed during the first post-operative week. The sheep were housed in stables with unlimited food and water. Six months after surgery, the animals were euthanized by intravenous injection of a lethal dose of pentobarbital (Dolethal[®], Vetoquinol, Lure, France).

Histology

After skin incision, the MBCP granules/fibrin materials and surrounding muscle tissue were harvested and immediately fixed in neutral buffered formalin solution for 24 h. The lumbar spine was also dissected from all animals and the fourth lumbar vertebrae were isolated and fixed in neutral buffered formalin solution for histomorphometrical analysis of the trabecular bone. After fixation, the intramuscular samples were dehydrated in an ascending series of graded ethanol (50, 70, 80, 95 and 100% with 24 h for each grade) and then in pure acetone for 48 h. The samples were finally impregnated for 5 days in methyl methacrylate (Prolabo) and embedded in polymethylmethacrylate (PMMA) resin. Blocks were cut roughly in order to eliminate excess PMMA and analyzed by X-ray micro-computed tomography (SkyScan μ -CT 1072, Belgium). The X-ray source was operated at a voltage of 100 kV and current of 98 μ A. The samples were rotated through 180° with a rotation step of 0.90°, an acquisition time of 5.6 s per scan and a pixel size of 11.8 μ m. Three-dimensional reconstructions were then performed using the software 3D Creator SkyScan. Each block was cut in half with a circular diamond saw (saw microtome 1600, Leica, Germany). One part was processed for histology while the other was used for histomorphometrical measurements. Sections measuring 100 μ m were made and observed with a polarized light microscope. Thin, 7 μ m sections were then prepared with a hard tissue microtome (Reichert-Jung, Supercut 2050, Germany) and stained with Movat's pentachrome [48]. For comparative purposes, four lumbar vertebrae were cut into rectangular samples (15 × 10 mm) containing only the trabecular bone of the vertebral body of the animal. The trabecular bone was then analyzed with X-ray micro-computed tomography (μ CT) in order to determine the number and thickness of the trabeculae.

Histomorphometrical analysis

The surface of the ceramic and mineralized bone was measured on cross-sectioned PMMA blocks by means of back-scattered electron microscopy (Leo 1450VP, Zeiss, Germany) and an image analysis system (Leica Quantimeter 5501 W, Japan). Prior to the SEM observations, the blocks were coated with gold-palladium at 20 mA for 4 min (EM Scope, UK). The SEM observations were made using secondary and back-scattered electrons (BSE) at 15 kV. The region of interest (ROI) was defined as the outer limit of the granules. The mineralized bone, MBCP ceramic granules and cellular areas were then measured on to contiguous BSE pictures using a semi-automatic image analyzer. The percentages of mineralized bone and ceramic were calculated by dividing their respective surface areas by that of the ROI. The volume of both the ceramic material and mineralized bone was measured using X-ray micro-computed tomography (μ CT) in the ROI. This method produced intergranular spaces and bone trabeculae in 3 dimensions. The ceramic granules and mineralized bone were distinguished on the basis of their respective gray levels. The corresponding volumes were measured and expressed as a percentage of the total implant volume (ROI). The number (Tb.N) and thickness (Tb.Th) of the bone trabeculae were measured in both the MBCP/fibrin glue. The same data were determined in the trabecular bone taken from the vertebrae of the same animals.

Statistical analysis

All data were expressed as averages and standard error. Differences were evaluated by variance analysis (ANOVA) with Fisher's probability least significant difference (PLSD) post-hoc test. The differences were considered significant at $p < 0.05$.

Results

Characterization of implant materials

Table 1 summarizes the chemical, physical and biological properties of the MBCP/fibrin composite. The composite material was composed of biphasic calcium phosphate granules and fibrin glue in a 2:1 volume ratio. SEM images of the MBCP/fibrin material are shown in Fig. 1. The MBCP granules showed macro- and microporosity in the 100–600 and <10 μ m range, respectively (Fig. 1a). As shown in Fig. 1b, the polymerized fibrin glue provided a 3 dimensional biological network of fibrin fibers with open porosity. Fig. 1c and d show the

Table 1 Chemical, physical and biological properties of MBCP/fibrin glue composite material

<i>Chemical composition</i>						
	HA (wt%) ^a	β -TCP (wt%) ^a	Ca/P ^a	CO ₃ ^b	CaO ^c	Specific surface area (m ² /g) ^e
MBCP	60 ± 2	40 ± 2	1.60 ± 0.02	No peaks	Negative	1.8 ± 0.1
<i>Physical properties</i>						
	Size of granules (mm)	Total porosity (%) ^d	Size of macro-pore ^d (μm)	Size of micropore ^d (μm)		
MBCP	1–2	70	450 ± 49	0.43 ± 0.2		
<i>Biological composition</i>						
	Fibrinogen concentration (mg/mL)	Thrombin concentration (UI)	Global porosity (%)	Reticulation time (s)		
Fibrin glue	100	4	60	60		

^a Analyzed by XRD

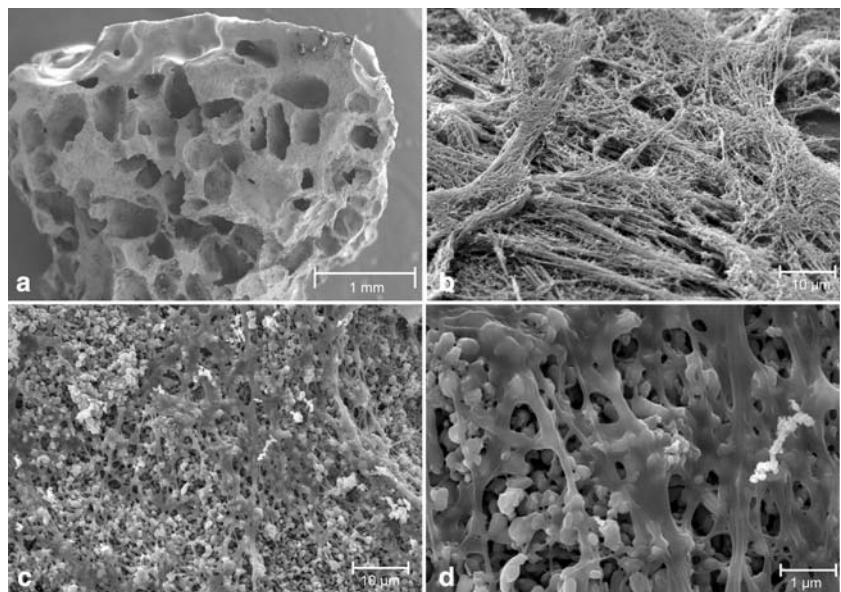
^b FTIR spectroscopy

^c CaO content tested by phenolphthalein

^d Analyzed by Hg porosimetry

^e Analyzed by BET

Fig. 1 SEM micrographs of the MBCP granules. **(a)** macropores, **(b)** micro-porous surface, **(c)** fibrin glue formed on to MBCP granules and **(d)** fibrin clot penetrating the micro-porous surface



composite made of MBCP granules and fibrin glue. After mixing with the MBCP granules, the fibrin glue provides cement between the ceramic granules and partially covered the ceramic material. The fibrin clot formed a complex network of fibers penetrating the microstructure of the granules. The clot was heterogeneous, with dense and narrowed mesh regions. After mixing the components, the reticulation of the fibrin glue was completed within 1 min and the composite material was ready to use and implanted into the sheep muscles.

Material osteogenesis

The osteogenic property of the MBCP/fibrin composite was studied in the lumbar muscles of sheep. About 2–3 cm³ of MBCP/fibrin composite were bilaterally implanted into the back muscles for 6 months. There was no detectable post-operative complication or implant rejection until euthanasia in any of the six animals. Macroscopically, the harvested MBCP/fibrin implants ($n = 12$) appeared firmly attached to the surrounding muscular tissues with signs of

neither inflammation nor fibrosis. All the samples were hard and rigid exhibiting numerous blood vessels.

Figure 2 shows histological sections of the MBCP/fibrin implants. Organized collagen fibers with abundant osteocytes and osteonal systems were clearly visible between the MBCP granules by using polarized light microscopy (Fig. 2a). The ectopic bone was in direct contact with the MBCP material. Mature bone tissue, with blood vessels, bridging three MBCP granules was observed on histological sections using Movat’s pentachrome staining. There was abundant mineralized bone in direct contact with the MBCP granules. The ectopic bone was surrounded by muscle tissue (Fig. 2b).

Back-scattered electron micrographs (BSE) of the MBCP/fibrin composite material are reported in Fig. 3. Only the MBCP ceramic granules and mineralized bone were noticeable. These two structures can easily be distinguished by their gray levels and morphology. As previously observed histologically, the ectopic bone appeared well-mineralized with numerous osteocytes and was directly apposited to the MBCP granules. Mineralized bone tissue was observed in the intergranular spaces bridging the MBCP granules as well as inside the macropores. Bone formation was limited to the implantation site and was not present in the surrounding muscle tissue. Bone distribution was not homogenous, with some formation on the edges as well as in the middle of the implant. Bone trabeculae

bridging the MBCP granules was what formed preferentially, while the inter-granular distance was less than 1 mm. As shown in Fig. 3b, an area with electron density similar to that of mineralized bone was sometimes observed on the surface of the MBCP granules. However, this area did not contain osteocytes and was not thus assigned to bone tissue. This area might have been caused by the precipitation of biological apatite onto the surface of the MBCP granules.

Figure 4 shows the micro-computed X-ray tomography of the MBCP/fibrin implants after intramuscular implantation for 6 months. In both the 3D image (Fig. 4a) and in the cross-section view (Fig. 4b), the MBCP ceramic granules appeared in orange while the mineralized bone was in light gray depending on their respective X-ray absorbance. Superposition of bone and ceramic gave a brown color. The newly formed bone appeared well distributed over the entire implantation site. Bone density was relatively uniform and substantial. As previously observed using BSE images, ectopic bone formation was associated with the MBCP granules forming bridges or trabeculae between themselves.

Table 2 summarized the histomorphometrical data calculated by using the BSE and μ CT methods for the MBCP/fibrin glue implants. The percentages of remaining bio-ceramic material and mineralized bone were measured over the region of interest by using both methods. The BSE

Fig. 2 Histology pictures of MBCP granules with fibrin glue after intramuscular implantation for 6 months in sheep back muscles. (a) Polarized light images showing mineralized bone with osteocytes (O) and Haversian (H) structures formed between the MBCP granules. (b) Histological images showing a bone trabecula between the MBCP granules (Movat’s pentachrome stain)

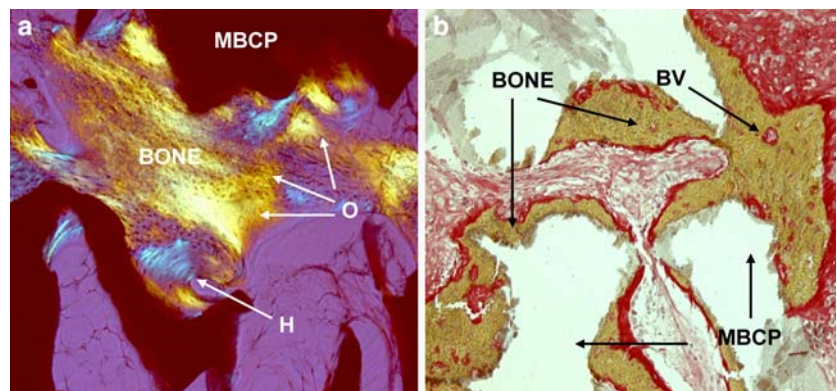


Fig. 3 BSE micrographs of MBCP/fibrin (a, b) after intramuscular implantation for 6 months in sheep back muscles. (Note the formation of well-mineralized bone with osteocytes lacunae. Ectopic bone formed between the MBCP granules and inside the macropores. White: MBCP granules, gray: bone and black: muscle tissue.)

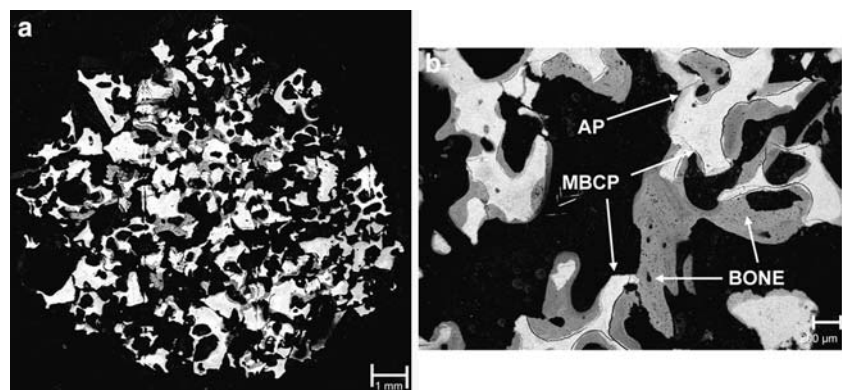


Fig. 4 Microscanner global view (a) and cross-section view (b) of MBCP/fibrin implants after intramuscular implantation for 6 months in sheep back muscles. Orange: MBCP granules, gray: bone and yellow: muscle tissue

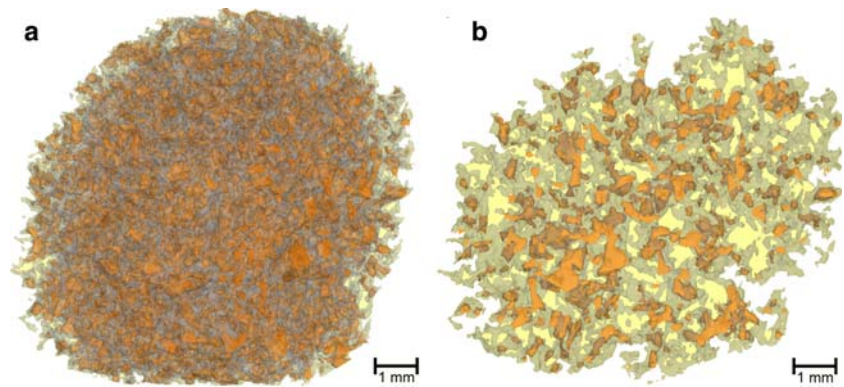


Table 2 Histomorphometrical data of the percentage of ceramic and ectopic bone for MBCP/fibrin implanted for 6 months into sheep muscles. Data were calculated from back-scattered electron microscopy (BSEM) and X-ray microtomography (μ CT)

Implants	BSEM/image analysis		X-ray microtomography	
	Ceramic (%)	Bone (%)	Ceramic (%)	Bone (%)
MBCP/fibrin (<i>n</i> = 12)	29.3 ± 5.9	6.7 ± 3.7	15.6 ± 4.7	17.0 ± 2.2

method gave a percentage of ceramic slightly higher than the μ CT method for the MBCP/fibrin implants. The same techniques gave an opposite tendency for the percentage of bone in the MBCP/fibrin composite materials. Irrespective to the method used, the quantity of ectopic bone and MBCP ceramic were about 12% and 25%, respectively.

Data concerning the architecture of the bone trabeculae formed between the MBCP granules are reported in Table 3. The average number and thickness of bone trabeculae on the implants were compared with those measured in the trabecular bone of sheep. The number and thickness of the trabeculae were around $15 \times 10^{-3} \mu\text{m}^{-1}$ and 216 μm for ectopic bone formed in the MBCP/fibrin implants. The data obtained for the structure of the ectopic bone formation were similar to the number ($16 \times 10^{-3} \mu\text{m}^{-1}$) and thickness

Table 3 Histomorphometrical data of the average number and thickness of the trabeculae in the ectopic bone after intramuscular implantation for 6 months of MBCP/fibrin. Data were obtained from μ CT and compared with measurements taken from the trabecular bone of sheep vertebra

Implants	Number of trabeculae (Tb.N) ($10^{-3} \mu\text{m}^{-1}$)	Thickness of trabeculae (Tb.Th) (μm)
MBCP/fibrin (<i>n</i> = 12)	15.6 ± 3.2	216 ± 32
Trabecular bone (<i>n</i> = 8)	16.1 ± 3.6	278 ± 40

(278 μm) of the trabeculae measured in the trabecular bone of the vertebral body ($p < 0.01$).

Discussion

Composite materials made of bioceramic and fibrin glue might be of interest in the reconstruction of bone defects. Calcium phosphate ceramics are currently used as bone substitutes in orthopedic, maxillo-facial or spinal surgery. However, bioceramics in the form of blocks or granules are not easy to implant in complex shaped bone defects. The addition of fibrin glue provides a biological liquid matrix that forms a gel around the ceramic granules to fit the anatomy of the bone defects [30]. Furthermore, the reconstruction of large bone defects requires osteogenic properties for the grafting material. In this study, the osteogenic property of the MBCP/fibrin glue composite implanted into the para vertebral muscles of sheep for 6 months was examined. We observed ectopic bone formation between the MBCP granules. Qualitatively, the bone tissue formed in the ectopic sites was well-mineralized, containing osteocytes and exhibiting Haversian structures. The quantity of ectopic bone and MBCP ceramic were about 12% and 25%, respectively. Bone occurred in contact and in between the MBCP granules forming trabeculae. The number and thickness of the trabeculae were comparable with those measured in spongy bone. Therefore, the MBCP/fibrin glue composite induced ectopic bone formation in muscles of sheep and thus, this novel composite material possesses osteogenic property.

Ectopic bone formation induced by materials has been described in previous studies [4, 5, 9–11, 31–36]. Osteoinduction by materials is a complex biological phenomenon that is not yet fully understood. It has been shown that ectopic bone formation is both material- and animal-dependent. Several studies have recently reported that specific materials are able to induce bone formation after implantation for 6–12 weeks in non-bony sites. For

instance, bone induction has been observed with synthetic hydroxyapatite ceramics, biphasic calcium phosphate ceramics, tricalcium phosphate ceramics, calcium phosphate cements, bioglass and even with titanium oxide and alumina ceramics implanted into the muscles of rabbits, dogs, goats, baboons and pigs [4–6, 11, 33, 34, 36, 37].

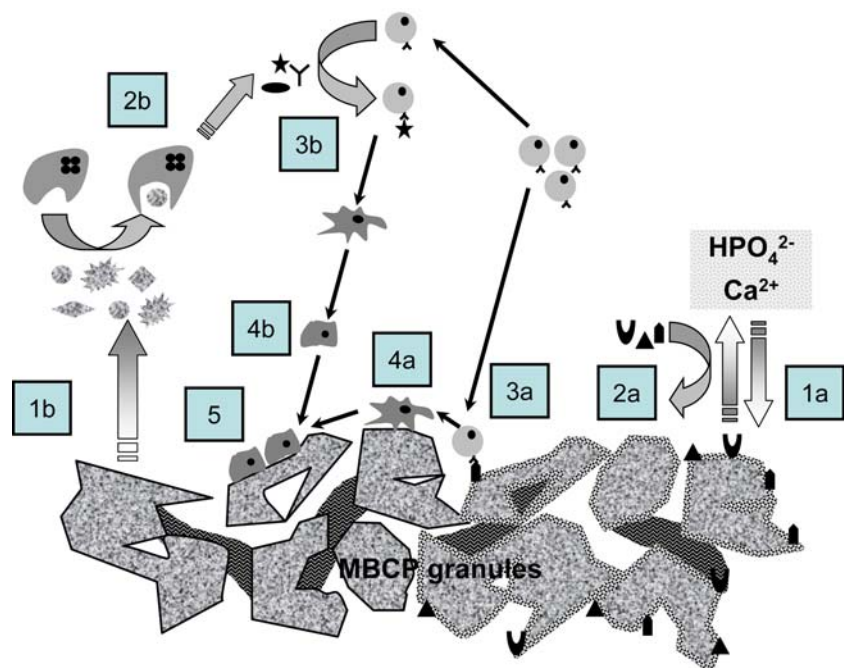
In our study, a composite made of MBCP granules and fibrin glue induced ectopic bone formation. Fibrin glue is well known for its properties regarding cell attraction, proliferation and differentiation in the wound healing process [29, 38–40]. Despite all these biological properties, only a few teams have studied the osteoinductive potential of fibrin glue after injection into non-bony sites [16, 41]. The results of these works have not made it possible to draw conclusions about the effect of fibrin glue on bone formation in ectopic sites. The formation of bone tissue is usually observed after 6–12 weeks in muscles [6, 42]. Nevertheless, the fibrin clot degraded within two weeks [29]. In this composite material, the fibrin glue may act just after the implantation of the composite biomaterial, at the early stage of ectopic bone formation. This early fibrin degradation does not preclude the possibility that some components of the fibrin glue are adsorbed on to the surface of the calcium phosphate granules and extend their action after fibrin degradation. Many components of the fibrin glue may be implicated in the process of ectopic bone formation (fibrinogen, thrombin, fibronectin) [43].

In osseous sites, bone formation occurs following two processes: endochondral or intramembranous ossification.

These two mechanisms are also observed when biomaterials are implanted into bone defects. Numerous studies have been performed with bone morphogenetic proteins (BMPs) loaded into collagen sponges and implanted into rodent muscles or subcutis [44, 45]. First, the BMPs usually induced cartilage tissue, which then transformed to bone tissue via the endochondral mechanism. Osteogenesis induced by materials is different from the process of bone formation induced by BMP-loaded materials where cartilage tissue and chondrocytes are generally observed prior to the formation of bone tissue. This endochondral ossification has been observed during embryogenesis. In previous studies and in the present work, neither cartilage tissue nor chondrocytes were observed but only mature bone tissue inside the bioceramics. Although only a late implantation time has been studied here, there is a consensus about direct bone formation inside calcium phosphate ceramics implanted into extra-skeletal sites [4, 46]. It is reasonable to consider that material osteogenesis follows the route of intramembranous ossification initiated by the presence and the differentiation of mesenchymal stem cells into osteoblastic cells.

It has been shown that surface microstructure plays a key role in the osteoinductive capacity of bioceramics [6]. Two possible mechanisms for osteoinduction by biomaterials are illustrated in Fig. 5. Both mechanisms were associated with the ceramic microstructure and both may have occurred at the same time. In the first hypothesis, the surface microstructure may promote both the precipitation of biological apatite and cell adhesion on to the surface of the materials. The micropores below 5 μm in diameter might greatly enhance ionic exchange with body fluids

Fig. 5 Diagram of possible mechanisms for material-induced osteogenesis. Following implantation, the MBCP granules partly dissolved (1a) and a biological apatite precipitated on to the surface of the MBCP concentrating endogenous bone growth factors (2a). Circulating stem cells were recruited by this surface (3a) and differentiated into osteoprogenitors (4a). Micro-particles detached from the micro-porous surface of MBCP (1b) and phagocytized by macrophages, which released inflammatory cytokines (2b). The inflammatory cytokines stimulated circulating stem cells (3b) to differentiate into osteoprogenitors (4b). Osteoblastic cells aligned and produced bone extracellular matrix on the MBCP (5)



and serve as nucleation sites for biological apatite precipitation [47]. Furthermore, the micropores greatly enlarge the surface area of the material and this may favor the adsorption and entrapment of endogenous proteins including BMPs, which have a high affinity for calcium phosphates [48]. These proteins on the surface of the material could promote both the adhesion and differentiation of progenitor cells into osteoblasts [49]. The second possible mechanism of biomaterial osteoinduction might be related to the release of micro particles. The microporosity of the MBCP was the result of a low temperature sintering (1,050 °C). Micro particles measuring <5 µm could be released around the biomaterial because of the dissolution of the inter grains in body fluids. This release of micro particles might provoke an inflammatory reaction [50, 51]. The local release of inflammatory cytokines might then stimulate circulating stem cells to differentiate into osteoblastic cells, thus producing bone tissue. This process could be similar to that observed during the healing of bone fractures by intra membranous ossification, where bone fragments are usually present. The degradation of the blood clot within a bone fracture might provoke a local inflammatory reaction leading to the release of cytokines. Those cytokines might in turn promote the differentiation of circulating stem cells into osteoblasts. In our study, the fibrin glue mixed with bioceramics might also provoke a cytokine release, which in turn promote the proliferation and differentiation of mesenchymal stem cells [26, 28].

Vascularization is also considered to be a crucial step in ectopic bone formation. Material osteogenesis has often been associated with the presence of capillary blood vessels inside bioceramic macropores. Blood vessels supply the oxygen, nutriment, signaling molecules and cells, which are the prerequisites for bone formation. Several studies have reported the benefits of fibrin glue on vascularization, blood vessel formation, wound healing and even osteogenesis [13, 15, 38, 52]. Fibrin glue mimics the final stage of blood clot formation. In addition, fibrin glue may ensure mechanical stability in the MBCP granules favorable to ectopic bone formation. In the present study, numerous blood vessels were observed both macroscopically and histologically. The blood vessels were observed in between the MBCP ceramic granules and near mineralized bone tissue. These blood vessels might be a source of progenitor cells, which can differentiate into osteoblasts under the stimulation of the inflammatory cytokines released by macrophages.

Conclusion

Ectopic bone formation was observed after the implantation of a composite material associating biphasic calcium

phosphate ceramic granules and fibrin glue into the back muscles of sheep for 6 months. The newly formed bone was in contact with the surface of the ceramic, appeared well-mineralized, forming trabeculae between the granules, and had characteristics similar to those of cancellous bone. However, the osteoinduction phenomena remain unclear and the biological effect of the fibrin during the biological events could not be observed. The addition of fibrin glue may facilitate the mechanical stability of the MBCP granules into complex shaped bone defects. The fibrin clot could also promote cell adhesion. The overall results indicated that MBCP/fibrin glue composite has osteoinductive properties. This composite could be used in bone tissue engineering with or without the addition of stem cells for reconstructive surgery.

Acknowledgements This study was supported financially by both the “Réseau National des Technologies pour la Santé” (RNTS 2002) and the “Contrat Etat Région” (CER Biomaterials). The authors would like to thank Baxter Bioscience for providing the fibrin glue (Tissucol) and Biomatlante for the biphasic calcium phosphate (TricoOs[®], Baxter BioSciences BioSurgery, Vienna Austria). We thank Stéphane Grolleau from the Institut des Matériaux de Nantes for measuring specific surface area and François Dulieu, Doctor in Veterinary Medicine, for collecting the µCT of vertebrae.

References

1. H. BURCHARDT, *Orthop. Clin. North Am.* **18** (1987) 187
2. T. BOYCE, J. EDWARDS and N. SCARBOROUGH, *Orthop. Clin. North Am.* **30** (1999) 571
3. G. DACULSI, O. LABOUX, O. MALARD and P. WEISS, *J. Mater. Sci. Mater. Med.* **14** (2003) 195
4. U. RIPAMONTI, J. CROOKS and A. KIRBRIDE, *South Africa J. Sci.* **95** (1999) 335
5. H. YUAN, M. VAN DEN DOEL, S. LI, C. A. VAN BLITTERSWIJK, K. DE GROOT and J. D. DE BRUIJN, *J. Mater. Sci. Mater. Med.* **13** (2002) 1271
6. P. HABIBOVIC, H. YUAN, C. M. VAN DER VALK, G. MEIJER, C. A. VAN BLITTERSWIJK and K. DE GROOT, *Biomaterials* **26** (2005) 3565
7. U. RIPAMONTI, *Clin. Orthop.* **269** (1991) 284
8. U. RIPAMONTI, *Biomaterials* **17** (1996) 31
9. H. YUAN, Y. LI, J. D. DE BRUIJN, K. DE GROOT and X. ZHANG, *Biomaterials* **21** (2000) 1283
10. H. YUAN, Z. YANG, J. D. DE BRUIJN, K. DE GROOT and X. ZHANG, *Biomaterials* **22** (2001) 2617
11. F. BARRERE, C. M. VAN DER VALK, R. A. DALMEIJER, G. MEIJER, C. A. VAN BLITTERSWIJK, K. DE GROOT and P. LAYROLLE, *J. Biomed. Mater. Res.* **66A** (2003) 779
12. D. M. ALBALA, *Cardiovasc. Surg.* **11**(Suppl 1) (2003) 5
13. J. M. KARP, F. SARRAF, M. S. SHOICHET and J. E. DAVIES, *J. Biomed. Mater. Res. A* **71** (2004) 162
14. L. LE GUEHENNEC, P. LAYROLLE and G. DACULSI, *Eur. Cell. Mater.* **8** (2004) 1; discussion 1
15. E. SOFFER, J. P. OUHAYOUN and F. ANAGNOSTOU, *Oral Surg. Oral Med. Oral Pathol. Oral Radiol. Endod.* **95** (2003) 521
16. S. ABIRAMAN, H. K. VARMA, P. R. UMASHANKAR and A. JOHN, *Biomaterials* **23** (2002) 3023
17. N. SCHWARZ, *Ann. Chir. Gynaecol. Suppl.* **207** (1993) 63

18. A. R. WITTKAMPF, *J. Craniomaxillofac. Surg.* **17** (1989) 179
19. G. DACULSI, M. BAGOT D'ARC, P. CORLIEU and M. GERSDORFF, *Ann. Otol. Rhinol. Laryngol.* **101** (1992) 669
20. R. E. KANIA, A. MEUNIER, M. HAMADOUCHE, L. SEDEL and H. PETITE, *J. Biomed. Mater. Res.* **43** (1998) 38
21. G. CUNIN, H. BOISSONNET, H. PETITE, C. BLANCHAT and G. GUILLEMIN, *Spine* **25** (2000) 1070
22. M. HALLMAN, A. CEDERLUND, S. LINDSKOG, S. LUNDGREN and L. SENNERBY, *Clin. Oral Implants Res.* **12** (2001) 135
23. D. CARMAGNOLA, T. BERGLUNDH and J. LINDHE, *J. Clin. Periodontol.* **29** (2002) 377
24. M. BAGOT D'ARC and G. DACULSI, *J. Mater. Sci. Mater. Med.* **14** (2003) 229
25. L. LE GUEHENNEC, E. GOYENVALLE, E. AGUADO, P. PILET, M. BAGOT D'ARC, M. BILBAN, R. SPAETHE and G. DACULSI, *J. Mater. Sci. Mater. Med.* **16** (2005) 29
26. R. S. SPITZER, C. PERKA, K. LINDENHAYN and H. ZIPPEL, *J. Biomed. Mater. Res.* **59** (2002) 690
27. O. GUREVICH, A. VEXLER, G. MARX, T. PRIGOZHINA, L. LEVDANSKY, S. SLAVIN, I. SHIMELIOVICH and R. GORODETSKY, *Tissue Eng.* **8** (2002) 661
28. Y. YAMADA, J. S. BOO, R. OZAWA, T. NAGASAKA, Y. OKAZAKI, K. HATA and M. UEDA, *J. Craniomaxillofac. Surg.* **31** (2003) 27
29. W. BENSaid, J. T. TRIFFITT, C. BLANCHAT, K. OUDINA, L. SEDEL and H. PETITE, *Biomaterials* **24** (2003) 2497
30. F. JEGOUX, E. GOYENVALLE, M. BAGOT D'ARC, E. AGUADO and G. DACULSI, *Arch. Orthop. Trauma Surg.* **125** (2005) 153
31. H. YAMASAKI and H. SAKAI, *Biomaterials* **13** (1992) 308
32. J. M. TOTH, K. L. LYNCH and D. A. HACKBARTH, *Bio ceramics* **6** (1993) 9
33. C. KLEIN, K. DE GROOT, W. CHEN, Y. LI and X. Zhang, *Biomaterials* **15** (1994) 31
34. Z. YANG, H. YUAN, W. TONG, P. ZOU, W. CHEN and X. ZHANG, *Biomaterials* **17** (1996) 2131
35. H. YUAN, Z. YANG, Y. LI, X. ZHANG, J. D. DE BRUIJN and K. DE GROOT, *J. Mater. Sci. Mater. Med.* **9** (1998) 723
36. D. LE NIHOANNEN, G. DACULSI, A. SAFFARZADEH, O. GAUTHIER, S. DELPLACE, P. PILET and P. LAYROLLE, *Bone* **36** (2005) 1086
37. P. HABIBOVIC, J. LI, C. M. VAN DER VALK, G. MEIJER, P. LAYROLLE, C. A. VAN BLITTERSWIJK and K. DE GROOT, *Biomaterials* **26** (2005) 23
38. D. J. GEER, D. D. SWARTZ and S. T. ANDREADIS, *Tissue Eng.* **8** (2002) 787
39. J. W. WEISEL, *Biophys. Chem.* **112** (2004) 267
40. R. R. PFISTER and C. I. SOMMERS, *Cornea* **24** (2005) 593
41. N. SCHWARZ, H. REDL, L. ZENG, G. SCHLAG, H. P. DINGES and J. ESCHBERGER, *Clin. Orthop. Relat. Res.* **293** (1993) 353
42. H. YUAN, J. D. DE BRUIJN, Y. LI, J. FENG, Z. YANG, K. DE GROOT and X. ZHANG, *J. Mater. Sci. Mater. Med.* **12** (2001) 7
43. G. LI, J. T. RYABY, D. H. CARNEY and H. WANG, *J. Orthop. Res.* **23** (2005) 196
44. M. GEIGER, R. H. LI and W. FRIESS, *Adv. Drug Deliv. Rev.* **55** (2003) 1613
45. M. YAMAMOTO, Y. TAKAHASHI and Y. TABATA, *Biomaterials* **24** (2003) 4375
46. H. YUAN, P. ZOU, Z. YANG, X. ZHANG, J. D. DE BRUIJN and K. DE GROOT, *J. Mater. Sci. Mater. Med.* **9** (1998) 717
47. G. DACULSI, R. Z. LEGEROS, M. HEUGHEBAERT and I. BARBIEUX, *Calcif. Tissue Int.* **46** (1990) 20
48. J. DE GROOT, *Tissue Eng.* **4** (1998) 337
49. S. A. KUZNETSOV, M. H. MANKANI, S. GRONTHOS, K. SATOMURA, P. BIANCO and P. G. ROBEY, *J. Cell. Biol.* **153** (2001) 1133
50. P. LAQUERRIERE, A. GRANDJEAN-LAQUERRIERE, E. JALLOT, G. BALOSSIER, P. FRAYSSINET and M. GUE-NOUNOU, *Biomaterials* **24** (2003) 2739
51. J. LU, M. C. BLARY, S. VAVASSEUR, M. DESCAMPS, K. ANSELME and P. HARDOUIN, *J. Mater. Sci. Mater. Med.* **15** (2004) 361
52. T. R. SANTHOSH KUMAR and L. K. KRISHNAN, *Biomaterials* **22** (2001) 2769